REPORT DOCUMENTATION PAGE

1. REPORT DATE *(DD-MM-YYYY)*	2. REPORT TYPE	3. DATES COVERED *(From - To)*
23 June 2017	Journal Article	05 January 2017 - 23 June 2017

4. TITLE AND SUBTITLE
DSMC Modeling of Flows with Recombination Reactions

5a. CONTRACT NUMBER

5b. GRANT NUMBER
N/A

5c. PROGRAM ELEMENT NUMBER
N/A

6. AUTHOR(S)
S. Gimelshein, I. Wysong

5d. PROJECT NUMBER
N/A

5e. TASK NUMBER
N/A

5f. WORK UNIT NUMBER
Q1MK

7. PERFORMING ORGANIZATION NAME(S) AND ADDRESS(ES)
Air Force Research Laboratory (AFMC)
AFRL/RQRC
10 E. Saturn Blvd.
Edwards AFB, CA 93524-7680

8. PERFORMING ORGANIZATION REPORT NUMBER

9. SPONSORING/MONITORING AGENCY NAME(S) AND ADDRESS(ES)
Air Force Research Laboratory (AFMC)
AFRL/RQR
5 Pollux Drive
Edwards AFB, CA 93524-7048

10. SPONSOR/MONITOR'S ACRONYM(S)
N/A

11. SPONSOR/MONITOR'S REPORT NUMBER(S)
AFRL-RQ-ED-JA-2017-011

12. DISTRIBUTION/AVAILABILITY STATEMENT
Approved for Public Release; Distribution Unlimited.
PA Case Number: 17092 Clearance Date: 14 February 2017
The U.S. Government is joint author of the work and has the right to use, modify, reproduce, release, perform, display, or disclose the work.

13. SUPPLEMENTARY NOTES

14. ABSTRACT
An empirical microscopic recombination model is developed for the direct simulation Monte Carlo method that complements the extended weak vibrational bias model of dissociation. The model maintains the correct equilibrium reaction constant in a wide range of temperatures by using the collision theory to enforce the number of recombination events. It also strictly follows the detailed balance requirement for equilibrium gas. The model and its implementation are verified with oxygen and nitrogen heat bath relaxation and compared with available experimental data on atomic oxygen recombination in argon and molecular nitrogen. Published by AIP Publishing.

15. SUBJECT TERMS
N/A

16. SECURITY CLASSIFICATION OF:			17. LIMITATION OF ABSTRACT	18. NUMBER OF PAGES	19a. NAME OF RESPONSIBLE PERSON
a. REPORT	b. ABSTRACT	c. THIS PAGE			I. Wysong
Unclassified	Unclassified	Unclassified	SAR	12	19b. TELEPHONE NUMBER *(Include area code)* N/A

DSMC modeling of flows with recombination reactions

Sergey Gimelshein[1,a)] and Ingrid Wysong[2]

[1]*ERC, Inc., Edwards AFB, California 93524, USA*
[2]*Aerospace Systems Directorate, AFRL, Edwards AFB, California 93524, USA*

An empirical microscopic recombination model is developed for the direct simulation Monte Carlo method that complements the extended weak vibrational bias model of dissociation. The model maintains the correct equilibrium reaction constant in a wide range of temperatures by using the collision theory to enforce the number of recombination events. It also strictly follows the detailed balance requirement for equilibrium gas. The model and its implementation are verified with oxygen and nitrogen heat bath relaxation and compared with available experimental data on atomic oxygen recombination in argon and molecular nitrogen. *Published by AIP Publishing.*
[http://dx.doi.org/10.1063/1.4986529]

I. INTRODUCTION

The direct simulation Monte Carlo (DSMC) method, pioneered by Bird over fifty years ago,[1] for most of that time has been considered the main numerical tool for modeling rarefied chemically reacting gas flows.[2,3] A number of chemical reaction models have been proposed over the years, from simple empirical ones such as the total collision energy (TCE) model[4] and the quantum kinetic (QK) model[5] to more complex approaches that include vibration coupling effects,[6–11] and to state-to-state and other sophisticated methods.[12,13,16] Due to scarce cross section or any other microscopic or non-equilibrium reaction data at the time, the main reference base for model validation used to be temperature dependent reaction rates. A model was usually developed from or checked versus available rates written in the Arrhenius format.[14] The primary focus for the model development so far has been dissociation and exchange reactions for diatomic, and sometimes for polyatomic, molecules. The recombination reaction was largely avoided in the DSMC computations, which to a significant degree is related to the area of application of the DSMC method.

This area is traditionally limited by the high computational cost of the DSMC method when applied to low Knudsen number flows, especially when these flows are three-dimensional.[15] Even for two-dimensional flows, modeling is usually conducted for Knudsen numbers $Kn > 0.001$, where the impact of recombination reactions is almost always minor, so that they may be either completely disregarded or modeled with a simple and not necessarily accurate model. In the last few years, however, the rarefied gas dynamics community has seen the development of efficient algorithms for modern computer architectures[16–19] which dramatically expand the area of practical applicability of the DSMC method. These methods have already been tested for reacting air flows.[20] Today, modeling of gas flows at Knudsen numbers as low as 10^{-4}, and possibly even lower, appears within reach.

Coincidentally, the development of high performance DSMC algorithms occurs at the time when significant push has been made towards increased accuracy of modeling of collision processes in reacting air (see, for example, Refs. 21–25). These studies, which mostly use molecular dynamics and quasiclassical trajectory (QCT) calculations, have provided detailed translational energy and internal level dependent cross sections, as well as non-equilibrium reaction rates, for oxygen and nitrogen dissociation and exchange reactions. Detailed QCT results for the specific reaction and known potential energy surface of interest always provide the highest accuracy when available and when the computational penalty of implementation can be overcome. As such, the cross-sectional information may be used directly in DSMC simulations,[12,13,16] although full scale translation-rotation-vibration energy tables would be prohibitively large and thus require some reduced models such as Ref. 26. Moreover, multi-dimensional hypersonic flow simulations still need fast and simplified models that capture the key physics and that can be used on reactions for which detailed QCT results are not available. In this case, newly available reaction data provide extensive basis for validation and analysis of empirical DSMC models.

An example of such a validation effort is the recent work,[27] where the extensive and high-quality recent quasiclassical trajectory calculation work from several groups on nitrogen molecule collisions with N[28,29] and N$_2$,[16,23] covering thermal non-elastic and dissociative processes, is used for DSMC model verification and parameter adjustment. Most widely used in the DSMC community models of dissociation reaction were considered.[27] The main conclusion was that the extended weak vibrational bias model[8,30] (called the bias model hereafter) provides the best agreement with benchmark vibrationally specific dissociation rates, while significant differences were observed for the other models. The bias model requires no *a priori* assumption of an Arrhenius rate coefficient, while providing realistic dissociation reaction rates in a wide range of temperatures.[8] It reproduces vibration-dissociation coupling, equilibrium, and nonequilibrium behavior as a natural consequence of

---

a)Electronic mail: gimelshe@usc.edu

its physics-based cross-sectional function and just a simple chemistry-based assessment of whether the reaction will be strongly favored or not. Our most recent analysis of nitrogen dissociation[27] has shown that the bias model provides good to excellent agreement with QCT non-equilibrium rates for oxygen dissociation reactions as well. The obvious advantage of the bias model is its ability to capture the vibration-dissociation coupling process, being at the same time easy to implement and numerically efficient. Moreover, it has the potential to be applied to reactive processes where no reliable non-equilibrium or equilibrium rates are known.

One significant disadvantage of the bias model is the lack of a compatible recombination model since the extension[30] to the weak vibrational bias model[8] has been provided only for the dissociation, but not for recombination, reactions. A compatible model in this case is a model that at minimum satisfies the principle of detailed balance for collisions in equilibrium gas, and at maximum also captures the corresponding equilibrium constant. This lack significantly limits the applicability of the bias model to near-continuum flows where the recombination reactions may be important, makes it difficult to provide comprehensive model validation and comparison with continuum approaches, and complicates its use in hybrid simulations. The recombination model that appears closest in terms of its compatibility to the bias model is the approach[8] developed for the original weak bias dissociation model. But even aside from the fact that the original[8] and extended[30] bias dissociation models differ, and a straightforward extension of the approach[8] to the extended bias model does not seem possible, the recombination strategy of Ref. 8 has several inherent deficiencies. These are the violation of the detailed balance requirement for the rotational mode, deviation from known equilibrium rate constants, and extremely difficult implementation.

Another possible route for the addition of the recombination to the bias model is a robust approach proposed in Ref. 31. *The approach[31] provides the way to sample post-recombination vibrational energies of newly created molecules. Its main idea is to record and tabulate vibrational energy distributions of dissociating molecules in equilibrium gas for a number of reference temperatures, so that for each reference gas temperature, there is a corresponding distribution function of vibrational levels of dissociating—and therefore recombining—molecules. The tabulation is conducted in a thermal bath prior to the DSMC flow modeling. Then, during the actual flow modeling, the pre-computed tables are used on a per-cell basis: each cell has its own temperature and thus uses its own part of the pre-computed table of vibrational distribution for recombining molecules.* Although the approach is developed for the TCE model[4] of chemical reactions and the Larsen-Borgnakke (LB) model[32] of internal energy transfer, it is likely extendable to other collision models. Inherent limitation of the approach is related to its reliance on equilibrium sampling. It may require prohibitively large tables in non-equilibrium conditions of different translational and internal temperatures, especially for quasisteady state conditions[23] with significantly underpopulated tail of the vibrational distribution.

The few other models[7,33,34] for recombination reactions in particle methods cannot be extended to complement the bias dissociation model, primarily due to the coupling of the vibrational mode with its dissociation probability. These models were developed for some specific dissociation models and cannot provide the detailed balance to the dissociation-recombination process when the bias model is used. For example, the early recombination models[33,34] were constructed for the TCE model[4] and used a simplified approach to the after-reaction energy redistribution, with no account for vibrational favoring in dissociation. The vibrationally favored dissociation (VFD) model[7] takes such a favoring into account but provides only a schematic description of recombination modeling and does not force the detailed balance. In addition, it is only suited to the corresponding dissociation model,[7] which has been shown[27,30] to be less robust and reliable than the bias model. The more recent recombination model[35] was designed in the quantum kinetic framework, and as such does not include vibration-dissociation favoring.

The main objective of this work is the development of a recombination model that complements the bias dissociation model and satisfies two key conditions: the number of recombination reactions at any given temperature is based on the correct recombination reaction rate, and the principle of detailed balance at equilibrium is taken into account. The first condition means that the recombination-dissociation process captures the known temperature dependence of the corresponding equilibrium constant, while the second condition implies that at equilibrium the number of molecules dissociating from any rovibrational state (J, v) is equal to the number of molecules recombining to that state.

The proposed approach to modeling the recombination process is straightforward to implement and may easily be adapted for most other DSMC dissociation models, such as quantum kinetic or total collision energy. Note that the present work, and all the related models referenced that consider simple 5-species air chemistry, operates within the simplifying assumption that considers only the ground electronic states of the molecular species. It is clear that in a more general case, particularly with ionization, excited electronic states will play an important role. Excited electronic states will greatly add to the complexity of dominant reaction mechanisms, including inverse predissociation and vibration-to-electronic energy transfer paths (see, for example, Ref. 36). The models mentioned in this work (whether implemented in DSMC or computational fluid dynamics, CFD) would need significant revisions in order to be considered for a flow where the latter processes are significant. However, the present development may be regarded as a step toward bridging the gap between the most accurate continuum CFD models that conventionally use both recombination and vibrationally favored dissociation processes in modeling hypersonic flows, and their kinetic counterparts, which often disregarded the recombination.

II. THE BIAS DISSOCIATION MODEL

The key objective of any DSMC chemistry model is to provide physically adequate number of reactions in the range of

temperatures of interest and, ideally, use reaction cross sections that provide good agreement with available experimental and theoretical data. Although it is possible to construct a temperature dependent algorithm for reaction modeling,[37] it appears natural for a particle approach, such as the DSMC method, to use the available information of translational and internal energies of colliding particles. This not only improves the physical realism of a model but also provides the opportunity to perform detailed microscopic verification and validation of the entire reaction process. The vast majority of the DSMC reaction models are therefore cross section and energy based,[3] and model the bimolecular reaction of dissociation of a molecule A_1A_2 consisting of atoms A_1 and A_2 and colliding with a particle X,

$$A_1A_2 + X \rightarrow A_1 + A_2 + X, \tag{1}$$
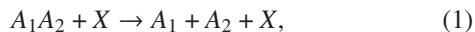
as a three-step process. First, upon selecting the collision pair A_1A_2 and X, it is checked whether the available collision energy E_c is large enough to exceed the reaction threshold E_d. Generally, the definition of E_c depends on the chosen dissociation model. In the original weak vibrational bias model,[8] it is assumed that E_c is the sum of the relative translational energy of the colliding pair, E_t, and the vibrational energy of the dissociating molecule A_1A_2, E_v, that is $E_c = E_t + E_v$. In the extended bias model,[30] $E_c = E_t + E_v + E_r$, where E_r is the rotational energy of A_1A_2.

If the available energy E_c is sufficient for dissociation, then the algorithm proceeds with its second step, which is the reaction probability P_d calculation and the acceptance or rejection of the colliding pair. The colliding pair is accepted for dissociation with a probability P_d which is always a function of the energies of the colliding pair. The actual form of the reaction probability is determined by the model used. In the weak vibrational bias model,[8] it is

$$P_d = A_d \left(1 - \frac{E_d - E_v}{E_t}\right) \exp\left[\lambda\left(\frac{E_v}{E_d} - 1\right)\right], \tag{2}$$

while in the extended bias model,[30]

$$P_d = A_d \left(1 - \frac{E_d - E_v}{E_t + E_r}\right) \exp\left(\lambda\left(\frac{E_v}{E_d} - 1\right)\right). \tag{3}$$

Here, A_d is the calibration constant chosen of order unity to match the known reaction rate constant of the given reaction, and λ is the parameter controlling the degree of vibrational favoring. Note that the reaction probabilities P_d are instantaneous and depend on the particular relative translational energy E_t of the colliding pair A_1A_2–X and the rotational and vibrational energies of molecule A_1A_2. Note also that the extended bias model provides better fit to known equilibrium and nonequilibrium reaction rates than the weak vibrational bias model[8] and other widely used DSMC models such as TCE and QK.[27] It was therefore chosen in this work as the baseline dissociation model.

The third, and final, step of the dissociation model is the transformation of the molecule A_1A_2 into atoms A_1 and A_2 and the energy redistribution over the reaction products. The energy redistribution in the bias model consists of the removal of E_d from the available energy E_c, and the sampling of the newly created atoms and third

particle velocities using the Larsen-Borgnakke mechanism[32] and the considerations of the energy and momentum conservation.

III. GENERAL PROCEDURE OF THREE-BODY RECOMBINATION

The inclusion in the reaction probability of the bias model of the rotational energy of the dissociating molecule, described in Sec. II, is necessary from the model accuracy perspective. However, it makes the recombination model[8] not suitable since the equations described in Sec. II E of Ref. 8 can no longer be used or extended in an analytic form. For example, the dependence of the dissociation cross section of the model[8] only on the vibrational and relative translational energies allows one to express the cross section σ_{fi} of a recombination into a vibrational level i from an initial free state f in a simple form

$$\sigma_{fi}(\epsilon) = \sigma_{el}(\langle\epsilon\rangle)P_{if},$$

where $\langle\epsilon\rangle$ is the symmetrized relative translational energy,[8] σ_{el} is the elastic collision probability, and P_{if} is the dissociation probability. While the approach has to rely on energy symmetrization,[38] it still provides an explicit expression for the stabilization of an orbiting pair of atoms into a specific vibrational state i.

Such an approach is not suitable in case the dissociation cross section also depends on the rotational state of dissociating molecules since both rotational and vibrational states of a molecule created after recombination need to be specified. It is however possible to use an efficient and straightforward procedure, described below, that allows one to satisfy the detailed balance requirement and at the same time capture the temperature dependence of the equilibrium constant, which was not enforced in Ref. 8. In this procedure, the process of recombination of two atoms, A_1 and A_2, into a molecule A_1A_2 is modeled as a two-step process of collisional stabilization of an orbiting complex (A_1A_2) by a third particle, X,

$$A_1 + A_2 \rightarrow (A_1A_2), \tag{4}$$

$$(A_1A_2) + X \rightarrow A_1A_2. \tag{5}$$
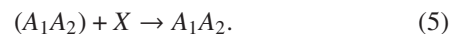
The model is built to satisfy two important constraints. First, the number of recombination reactions at any given temperature needs to be based on the correct recombination reaction rate, which is determined as the ratio of the corresponding dissociation rate of the bias model to the equilibrium constant specific to the dissociating/recombining molecular species. Second, the model must take into account the principle of detailed balance, which states that at equilibrium the forward rate for each elementary process is equal to the reverse rate of that process. Applied to the bias model, that principle implies that the number of molecules dissociating from any rovibrational state (J, v) is equal to the number of molecules recombining to that state.

The proposed recombination algorithm may be used as an addition to any conventional DSMC collision scheme, such as the majorant frequency scheme[39] or the no time counter scheme.[2] It is added to the cell-based atom-atom elastic

collision algorithm, and the complete procedure that includes the conventional elastic collision and recombination reaction related steps is as follows.

1. The first step is the conventional DSMC elastic collision procedure for atom-atom interactions. In this procedure, two atoms are selected randomly from all atoms located in that cell. The number of pair selections N_s is determined by the collision frequency in the given cell, which in turn depends on the atom-atom intermolecular potential as well as the time step Δt and the number density n and the number of simulated atoms N of colliding atomic species A_1 and A_2,

$$N_s = \varepsilon n_{A_1} N_{A_2} (\sigma_T g)_{max} \Delta t.$$

   Here, $\varepsilon = 0.5$ for $A_1 = A_2$ and 1 otherwise, σ_T is the total collision cross section, and g is the relative collision velocity. The subscript *max* denotes the maximum value for the given cell. The selected pair of atoms is accepted for collision or rejected based on its relative collision velocity $g_{A_a A_2}$ and the selected intermolecular potential, such as variable hard sphere (VHS) or variable soft sphere (VSS).[2,8] Typically, the acceptance probability is $P_a = \frac{(\sigma_T g)_{A_1 A_2}}{(\sigma_T g)_{max}}$.

2. If atoms A_1 and A_2 are accepted for physical collisions, then either an elastic collision or a recombination reaction is possible. The probability of recombination is P_r, and the probability of elastic collision is $1 - P_r$. Here, P_r is a function of the relative collision energy $E_t r(A_1, A_2)$ of pair A_1, A_2, computed to match the equilibrium constant as discussed below. Note that only two outcomes are considered in this work for atom-atom interactions, an elastic collision and a recombination. A selection method such that of Ref. 40 may be used if other reactive mechanisms need to be included.

3. If $\mathcal{R} < P_r$, where $\mathcal{R}$ is the random number uniformly distributed in the interval (0, 1), then there should be a recombination reaction between atoms A_1 and A_2. In this case, the internal (rotational J and vibrational v) energy states of the newly created molecule $A_1 A_2$ are chosen from the list of states of recently dissociated molecules. The internal states of recombining molecules are assigned sequentially from the local list, as described in detail in Sec. VI. Importantly, such a procedure, along with the balanced numbers of dissociation and recombination reactions, governed by the local equilibrium rates, naturally satisfies the microscopic reversibility principle.[41]

4. Third particle X is picked randomly from all particles in the spatial cell, and the new velocities of X and $A_1 A_2$ are calculated using the VHS/VSS algorithm with the conservation of momentum and energy.

For this algorithm to be fully defined, we need to specify the energy form of the reaction probability P_r and the rule for the selection of internal energy levels of the newly created molecule. As discussed below, the detailed balance is explicitly used for the latter, while the collision theory for chemical reactions is applied to find P_r. To apply the collision theory so

that the reaction equilibrium constant is captured, it is necessary to present the dissociation and recombination rates in an extended Arrhenius form.[42]

IV. DISSOCIATION AND RECOMBINATION RATES OF THE BIAS MODEL

The energy dependent probability of the bias dissociation model is simple and straightforward to implement, but it does not allow its exact analytic integration to provide equally simple temperature dependent reaction rate constant. This is mostly due to the discrete internal energy modes since the integral over the relative velocities is complemented by the summation over rotational and vibrational levels. Note that while the discrete rotational mode may be replaced by its continuous analog, the vibrational mode cannot be simplified this way due to large energy spacing between low vibrational levels. Also note that even fully continuous internal modes would not allow one to reduce the bias model dissociation rate to the extended Arrhenius form of $AT^B e^{\frac{-E_d}{kT}}$.

Even though the closed analytic form for the bias model is not available, the equilibrium reaction rates obtained by this model may be fairly accurately approximated by a temperature dependence written in the Arrhenius form. This is illustrated in Fig. 1 for the $N_2 + N \rightarrow N + N + N$ dissociation reaction. In this figure, the calculated rate of the bias model was based on Eq. (3). The constants A_d, B_d, and E_d of the Arrhenius equation, $AT^B e^{\frac{-E_d}{kT}}$, which provide the best fit to the calculated bias model dissociation rates in the temperature range between 3000 K and 20 000 K are listed in Table I, along with the recommended constants of the bias model A_d and λ. Here, the reaction rate constants are in m^3/(molecule/s), and the ratio of the dissociation energy threshold to the Boltzmann constant E_d/k is in K. Figure 1 shows that the Arrhenius form approximates the calculated rate very well, with the maximum error in the considered temperature range not exceeding 5% (and typically less than 2%). The approximation is almost as good for the other dissociation reactions of air species, also listed in Table I.
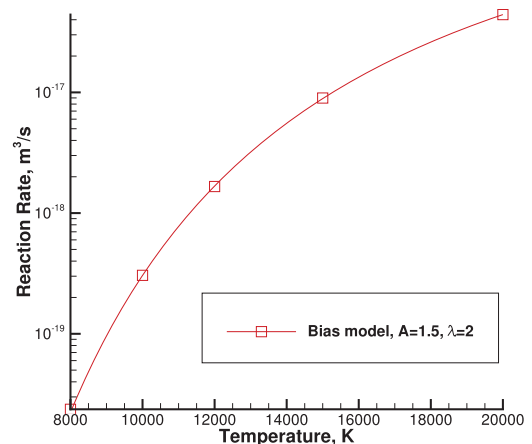

FIG. 1. Reaction rate for $N_2 + N \rightarrow N + N + N$ dissociation. Symbols—calculated rate, line—its Arrhenius approximation.

TABLE I. Arrhenius reaction constants matching the bias model rates for different dissociation reactions.

Reaction	A_i	λ	A_d	B_d	E_d/k
$N_2 + N \rightarrow N + N + N$	1.5	2	2.56×10^{-10}	−1	113 400
$N_2 + N_2 \rightarrow N + N + N_2$	1.5	4	8.28×10^{-11}	−1	113 400
$O_2 + O \rightarrow O + O + O$	4	2	1.83×10^{-10}	−1	59 370
$O_2 + O_2 \rightarrow O + O + O_2$	2	4	4.093×10^{-11}	−1	59 370
$O_2 + Ar \rightarrow O + O + Ar$	0.25	2	1.17×10^{-11}	−1	59 370
$O_2 + N_2 \rightarrow O + O + N_2$	0.4	2	2.50×10^{-11}	−1	59 370

TABLE II. Constants in the recombination reaction rates for the bias model. The units of the recombination rate constant are m^6/(molecules^2/s).

Reaction	A_r	B_r
$N_2 + N \rightarrow N + N + N$	2.36×10^{-41}	−1
$N_2 + N_2 \rightarrow N + N + N_2$	7.64×10^{-42}	−1
$O_2 + O \rightarrow O + O + O$	2.53×10^{-43}	−0.5
$O_2 + O_2 \rightarrow O + O + O_2$	5.66×10^{-44}	−0.5
$O_2 + Ar \rightarrow O + O + Ar$	1.62×10^{-44}	−0.5
$O_2 + N_2 \rightarrow O + O + N_2$	3.46×10^{-44}	−0.5

The equilibrium constants used in this work follow the recommendations of Ref. 42 for the temperature range between 3000 K and 8000 K, with the nitrogen and oxygen equilibrium constants $K_e^{N_2}$ and $K_e^{O_2}$ written as

$$K_e^{N_2} = 1.084 \times 10^{31} e^{-113\,400/T} \text{molecule/m}^3, \quad (6)$$

$$K_e^{O_2} = 7.227 \times 10^{32} T^{-0.5} e^{-59\,370/T} \text{molecule/m}^3. \quad (7)$$

The recombination reaction rate constant k_r is then obtained as the ratio of the corresponding dissociation rate k_d to the equilibrium constant K_e and may be presented in the form

$$k_r = A_r T^{B_r}. \quad (8)$$

The constants A_r and B_r are listed in Table II. Here, the dimensions of the recombination constant A_r are m^6/(molecule^2/s). In what follows, the rates from Tables I and II are used except where indicated otherwise.

V. RECOMBINATION REACTION PROBABILITY

As soon as the recombination reaction rate is written in the Arrhenius form of Eq. (8), the recombination probability may be calculated based on the collision theory for chemical reactions, and its derivation generally follows the procedures outlined in Refs. 33 and 34. The main goal here is to define a recombination probability, P_r, which provides the number of

collisions that at equilibrium follows the recombination rate listed in Sec. IV, and thus allows one to match the equilibrium constant at thermochemical equilibrium.

The rate of change of atomic species A_1 due to recombination

$$A_1 + A_2 + X \rightarrow A_1 A_2 + X \quad (9)$$
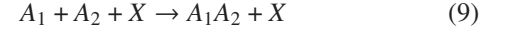
may be written as

$$-\frac{dn_{A_1}}{dt} = n_{A_1} n_{A_2} n_X k_r, \quad (10)$$

where n is the number density of the corresponding species. The recombination rate k_r is written as

$$k_r = \int \cdots \int c_r^{(3)} \sigma_r^{(3)} f(\bar{v}_{A_1}) f(\bar{v}_{A_2}) f(\bar{v}_X) d\bar{v}_{A_1} d\bar{v}_{A_2} d\bar{v}_X, \quad (11)$$

where $c_r^{(3)}$ and $\sigma_r^{(3)}$ are the relative velocity and reaction cross section for the three-body collision, respectively, f is the molecular velocity distribution function, and $\bar{v}$ is the velocity. The molecular velocities have X, Y, and Z components, and thus the integral is nine-fold. Note that the three-body recombination reaction cross section $\sigma_r^{(3)}$ has the dimensions of m^5/molecules^2 (see Ref. 43).

Since the main requirement imposed on the model is matching the equilibrium rate, hereafter we will assume the Maxwellian form of the distribution function f. It is also assumed that the recombination probability depends on the relative velocity of colliding atoms, c_r, but not on the velocity of the third particle X. This is reasonable since the internal states of the recombining molecules are selected from the detailed balance considerations independent of the relative collision velocities (see Sec. VI). Note also that at equilibrium, $c_r^{(3)}$ can be expressed as a function of the ordinary two-body relative velocity c_r and the masses of the colliding particles.[43] In this case, one can take the integration over $c_r^{(3)}$ and $\sigma_r^{(3)}$ out of the integral over $\bar{v}_X$, and simplify the product as

$$\int_{-\infty}^{\infty} c_r^{(3)} \sigma_r^{(3)} f(\bar{v}_X) d\bar{v}_X = M c_r \frac{\sigma_r}{n_X} = \frac{P_r}{n_X} c_r \sigma_{tot}(c_r). \quad (12)$$

Here, M is a mass-dependent constant that relates $c_r^{(3)}$ and c_r,[43] $\sigma_{tot}(c_r)$ is the atom-atom total collision cross section, which in this work is defined by the VHS/VSS intermolecular potential, and P_r is the recombination probability, which is conventionally the ratio of the reactive to total collision cross section, and in this case also includes the constant M.

Then, substituting Eq. (12) into Eq. (11), and changing the variables $\bar{v}_{A_1}$ and $\bar{v}_{A_2}$ to the center of mass velocity c_{cm} and the relative velocity c_r, as discussed in Sec. IV C of Ref. 2, for the flow at equilibrium, we have

$$k_r = \int \cdots \int \frac{P_r}{n_X} c_r \sigma_{tot}(c_r) f(\bar{v}_{A_1}) f(\bar{v}_{A_2}) d\bar{v}_{A_1} d\bar{v}_{A_2} = \frac{2(m_{A_1} m_{A_2})^{\frac{3}{2}}}{\pi(kT)^3} \int_{-\infty}^{\infty} c_{cm}^2 e^{-\frac{(m_{A_1}+m_{A_2})c_{cm}^2}{2kT}} dc_{cm} \int_{-\infty}^{\infty} \frac{P_r}{n_X} \sigma_{tot}(c_r) c_r^3 e^{-\frac{m_r c_r^2}{2kT}} dc_r$$

$$= \frac{2(m_{A_1} m_{A_2})^{\frac{3}{2}}}{\pi(kT)^3} \left(\frac{2kT}{m_{A_1} + m_{A_2}}\right)^{\frac{3}{2}} \frac{\sqrt{\pi}}{4 n_X} \int_0^{\infty} P_r c_r^3 \sigma_{tot}(c_r) e^{-\frac{m_r c_r^2}{2kT}} dc_r, \quad (13)$$

where m_r, m_{A_1}, and m_{A_2} are the reduced mass and the masses of atoms A_1 and A_2, respectively.

The primary unknown in this expression is the reaction probability, P_r. Let us now recall the functional dependence of the recombination reaction rate at equilibrium, Eq. (8). Since the rate written in Eq. (13) for equilibrium conditions needs to be equal to $A_r T_r^B$, it is reasonable[33,34] to assume the relative velocity dependent form of P_r as

$$P_r = \Phi c_r^{\Psi}, \tag{14}$$

where Φ and Ψ are constants to be found by equating the right hand sides of Eqs. (8) and (13).

For the VHS/VSS intermolecular potentials, the total collision cross section is[2]

$$\sigma_{tot} = \pi d_{ref}^2 \left(\frac{2kT_{ref}}{m_r c_r} \right)^{\alpha} \frac{1}{\Gamma(2 - \alpha)}. \tag{15}$$

Here, Γ is the gamma-function, d_{ref} and T_{ref} are the reference diameter and temperature of the VHS/VSS models, respectively, and α is the exponent in the viscosity-temperature dependence, $\mu \propto T^{0.5+\alpha}$. For hard sphere and Maxwell molecules, α is 0 and 0.5, respectively.

We also need to recall that the number of collisions N_{coll} between atomic species A_1 and A_2, calculated in any given collision cell, is proportional to the product of species number densities as

$$N_{coll} \propto \frac{n_{A_1} n_{A_2}}{\epsilon},$$

where the constant ϵ related to the number of unique pairs is 2 when $A_1 \equiv A_2$, and 1 otherwise. This constant needs to be accounted for when finding the reaction probability P_r from Eq. (13).

Then, taking into consideration ϵ and substituting Eq. (15) into Eq. (13),

$$k_r = \frac{4}{\epsilon\sqrt{\pi}} \left(\frac{m_r}{2kT} \right)^{\frac{3}{2}} \left(\frac{2kT_{ref}}{m_r} \right)^{\alpha} \frac{\pi d_{ref}^2}{\Gamma(2 - \alpha)} \frac{\Phi}{n_X}$$
$$\times \int_0^{\infty} c_r^{3-2\alpha+\Psi} e^{-\frac{m_r c_r^2}{2kT}} dc_r. \tag{16}$$

To integrate Eq. (16), it is convenient to change variables from relative velocity of colliding atoms c_r to relative collision energy E_r, $E_r = \frac{m_r c_r^2}{2}$, so that the integral in that equation becomes

$$\int_0^{\infty} c_r^{3-2\alpha+\Psi} e^{-\frac{m_r c_r^2}{2kT}} dc_r = \frac{1}{2} \left(\frac{2}{m_r} \right)^{2-\alpha+\frac{\Psi}{2}} \int_0^{\infty} E_r^{1-\alpha+\frac{\Psi}{2}} e^{\frac{-E_r}{kT}} dE_r = \frac{1}{2} \left(\frac{2kT}{m_r} \right)^{2-\alpha+\frac{\Psi}{2}} \int_0^{\infty} \left(\frac{E}{kT} \right)^{1-\alpha+\frac{\Psi}{2}} e^{-\frac{E_r}{kT}} d\frac{E_r}{kT}$$

$$= \frac{1}{2} \left(\frac{2kT}{m_r} \right)^{2-\alpha+\frac{\Psi}{2}} \Gamma\left(2 - \alpha + \frac{\Psi}{2} \right). \tag{17}$$

From Eqs. (16) and (17), we can find the final expression for the reaction rate constant,

$$k_r = \frac{2}{\epsilon\sqrt{\pi}} \frac{\Gamma\left(2 - \alpha + \frac{\Psi}{2} \right)}{\Gamma(2 - \alpha)} \pi d_{ref}^2 \frac{\Phi}{n_X} \left(\frac{2kT}{m_r} \right)^{0.5-\alpha+\frac{\Psi}{2}} \left(\frac{2kT_{ref}}{m_r} \right)^{\alpha}. \tag{18}$$

The constants Φ and Ψ in the recombination probability of Eq. (14) are found by equating the right hand sides of Eqs. (8) and (18) and the exponents in the temperature dependence,

$$\Phi = \frac{\epsilon\sqrt{\pi}}{2} \frac{\Gamma(2 - \alpha)}{\Gamma\left(2 - \alpha + \frac{\Psi}{2} \right)} \frac{A_r n_X}{T_{ref}^{\alpha} \pi d_{ref}^2} \left(\frac{m_r}{2k} \right)^{\frac{1+\Psi}{2}}, \tag{19}$$

$$\Psi = 2B_r + 2\alpha - 1.$$

The reaction probability of Eq. (14) is thus defined and may be used explicitly in the DSMC simulation.

VI. INTERNAL ENERGY STATES OF MOLECULES CREATED IN RECOMBINATION

The second most important constraint, after modeling the number of recombination events which preserves the equilibrium constant, is satisfying the principle of detailed balance at equilibrium. Note that this is especially critical for the vibrationally favored dissociation model such as the bias model used here. If the number of molecules that dissociate from a particular vibrational level v will not be equal to the

number of molecules that populate that level after recombination, then the vibrational distribution function will deviate from its Boltzmann form, and maintaining correct forward and reverse reaction rates at equilibrium will not be possible. The main idea of the proposed approach is for each spatial cell to record the rotational and vibrational levels of molecules that dissociated in that cell and assign them to molecules created after recombination.

The following scheme is proposed that strictly satisfies the detailed balance requirement. First, the rotational and vibrational levels of dissociating molecules are recorded in two dedicated 2D arrays, one for rotational and the other for vibrational levels (although those may be combined in a single array if needed). The arrays are cell-based, which means that each spatial cell has its own list of rotational and vibrational levels of dissociated molecules. The first array dimension is therefore dedicated to the spatial cells, and the second dimension is the memory depth (how many of the most recently dissociating molecules will be remembered). Calculations have shown that the memory depth does not have to be large; typically, storing only five rotational and vibrational levels in each cell is sufficient. Then, only the levels of the last five dissociated molecules are stored, the levels of molecules that dissociated earlier are discarded. The arrays are filled sequentially, and when the corresponding cell-based running counter exceeds the array's maximum length (the memory depth), it returns to the first element of the array, overriding the values stored earlier.

The lists of stored rotational and vibrational levels of dissociated molecules are used to populate the internal states of molecules created after recombination. A cell-based counter is increased by one every time a pair of atoms is accepted for recombination, and rotational and vibrational levels, J and v, which correspond to the value of that counter, are selected from the stored list. Note that in recombination dominated flows, there may be cells where the recombination starts before dissociation, so that initially there are no internal energy lists of dissociated molecules. In this case, one can take into consideration the functional dependence of the dissociation probability of the bias model, and consider only its dominant exponential term for the reverse process of recombination. In this case, the distribution function of vibrational energy E_v of newly created molecules may be approximated as

$$f(E_v) = \frac{\lambda}{e^\lambda - 1} e^{\lambda \frac{E_v}{E_d}}.$$

The vibrational energy then sampled as

$$E_v = \frac{E_d}{\lambda} \ln(1 + \mathcal{R}(e^\lambda - 1)), \qquad (20)$$

where $\mathcal{R}$ is the random number uniformly distributed between 0 and 1. After that, the vibrational level v of the new molecule is set to the maximum value for which energy does not exceed E_v, and the rotational level is set not to exceed the remaining energy. Although the procedure of Eq. (20) only approximates the detailed balance, it is used only until the first dissociation and thus has no negative effect for steady state flows, and negligible effect for transient recombination dominated flows, as shown in Sec. VIII.

The after-recombination velocities of particles $A_1 A_2$ and X are computed in two steps that provide momentum and energy conservation. At the first step, the velocity of molecule $A_1 A_2$ is set to the center of mass velocity of the system of two atoms A_1 and A_2, as dictated by the conservation of momentum requirement. The relative translational energy between particles $A_1 A_2$ and X is then

$$E_t^{A_1 A_2 - X} = E_t^{(A_1 A_2) - X} + E_t^{A_1 - A_2} - E_r(J) - E_v(v) - E_d. \quad (21)$$

Here, $E_t^{(A_1 A_2) - X}$ is the relative translational energy of the center of mass of the orbiting pair $(A_1 A_2)$ and the third particle X, $E_t^{A_1 - A_2}$ is the relative translational energy of the two atoms, and $E_r(J)$ and $E_v(v)$ are the rotational and vibrational energies of levels J and v, respectively. Note that for some J, v, and $E_t^{(A_1 A_2) - X}$, the value of $E_t^{A_1 A_2 - X}$ may be less than 0. In this case, another particle X needs to be randomly selected from all particles in the cell, while the selected levels J and V should not be changed. Alternatively, all three particles A_1, A_2, and X may be re-selected.

At the second step, the final velocities of $A_1 A_2$ and X are calculated using the conventional VHS or VSS algorithm[2] for the relative translational energy $E_t^{A_1 A_2 - X}$.

VII. VERIFICATION OF THE RECOMBINATION MODEL

A. Detailed balance at thermal and chemical equilibrium

For any dissociation model, the verification of the corresponding recombination model is fairly straightforward:

one needs (i) to verify that the model is capable of maintaining thermochemical equilibrium with the reactant mole fractions that correspond to the given equilibrium constant, in a wide range of temperatures and pressures, and (ii) check that the system that was initially at non-equilibrium converges to the correct equilibrium condition. Equilibrium here needs to be both microscopic (Maxwellian velocity distributions and Boltzmann internal energy populations) and macroscopic (equal mode temperatures and the ratio of species mole fractions matching the equilibrium constant).

With this in mind, the first set of tests was conducted for a system initially at full thermal and chemical equilibrium, with the concentrations of molecular and atomic species set to their equilibrium value at a given temperature and with the Maxwell-Boltzmann distribution of particle velocities and internal energies at that temperature. The SMILE DSMC code[44] was used in all computations, extended to include the proposed bias model. The calculations were conducted for N_2–N, O_2–O, and O_2–O–Ar systems, with dissociation-recombination reactions $N_2 + M \leftrightarrow N + N + M$ and $O_2 + M \leftrightarrow O + O + M$, where M is the third particle that can be of any species of the gas mixture. Modeling results in an adiabatic reservoir with the specular gas-surface interaction, gas temperature varying from 3000 K to 14 000 K, and pressures from 0.01 to 50 atm have indicated that the bias dissociation and recombination model does not disturb an equilibrium system. The observed deviation from equilibrium constant was less than 0.3%. That deviation, aside from the statistical scatter on the order of 0.1%, was also due to the 1%–2% difference between the actual dissociation rates for the bias model and their approximation written in the Arrhenius form.

An example of thermal relaxation from the equilibrium state is shown in Fig. 2(a), where the translational and internal temperatures (T_{trn}, T_{rot}, and T_{vib}) and the species mole fractions (X[O] and X[O_2]) are shown as functions of time. The system is O_2–O, the initial temperature is 5000 K, and the number density is 2×10^{25} molecule/m^3, with the mole fractions of 81.4% O–18.6% O_2. The total number of simulated molecules in the system was approximately ten million, the total relaxation time amounted to about 10 000 mean collision times, and the number of dissociation and recombination reactions during the relaxation time exceeded two million. The figure clearly shows that the system does not deviate from its initial state. The distribution functions are equilibrium, as illustrated in Fig. 2(b) for the vibrational (VDF) and rotational (RDF) distribution functions.

B. Relaxation from a chemically non-equilibrium state

The second set of tests, also conducted for the above three gas systems, was aimed at the verification of the ability of an initially non-equilibrium system to reach equilibrium. With varying initial gas pressures, temperatures, and compositions, the system was tracked until the steady state is reached, and then the velocity and energy distribution functions and species mole fraction were compared to the corresponding equilibrium values. An example of the temporal relaxation of a non-equilibrium system is presented in Fig. 3(a) for a
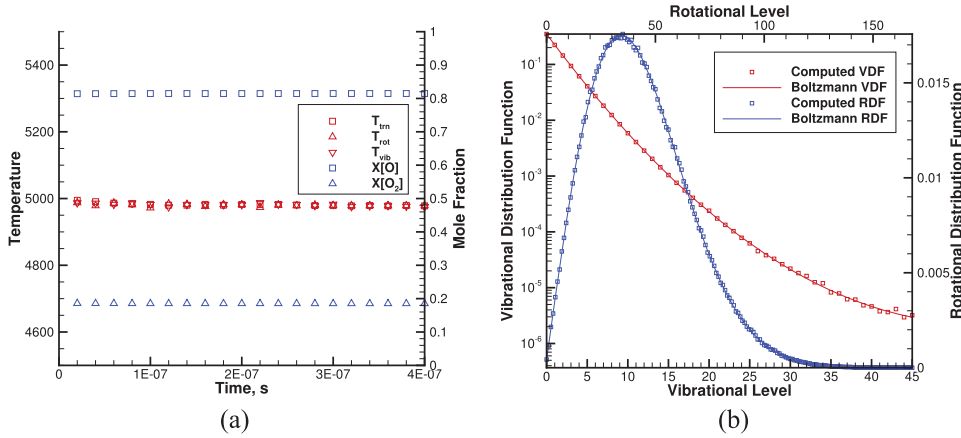
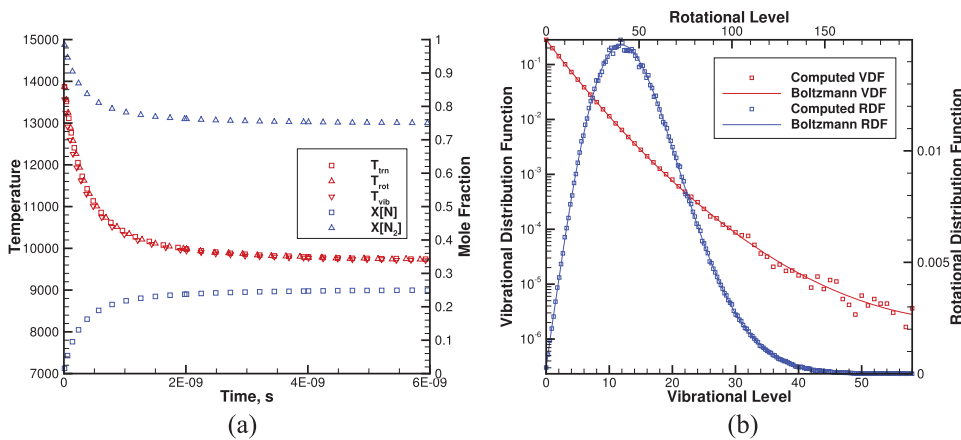FIG. 2. Equilibrium relaxation in O_2-O bath: macroparameters (left) and internal energy distribution functions (right).

FIG. 3. Collisional relaxation toward equilibrium state (left) and internal energy distribution functions at 6 ns (right). N_2-N thermal bath.

N_2-N gas mixture. Initially, the gas is 100% N_2 with a temperature of 14 000 K in all modes and a number density of 10^{27} molecule/m^3. The collisional relaxation results in a preferential dissociation in the first nanosecond, followed by slow relaxation toward thermochemical equilibrium. The equilibrium is reached at about 6 ns. The internal energy level populations at that time become fully equilibrium, as illustrated in Fig. 3(b).

VIII. RECOMBINATION MODEL VALIDATION

Chemistry model validation is traditionally difficult for kinetic methods, mostly due to limited availability of experimental data in near-continuum flow regimes where kinetic, non-equilibrium effects would be pronounced. Validation is even more challenging for recombination models since most shock tube data, being the primary scope of DSMC studies dealing with dissociation and exchange reactions, are dissociation-dominated, and the impact of recombination is relatively minor and generally too small for detailed validation. In this work, we have chosen ozone pyrolysis[45] and photolysis[46] experiments where the ozone molecules are quickly transformed to oxygen atoms, which then recombine through collisions with the surrounding gas to produce molecular oxygen. In the first case,[45] pyrolysis of ozone was used to produce an excess of O atoms in the shock tube, and oxygen collisional recombination then proceeded in a thermal bath of

argon heated to temperatures between 2000 K and 3000 K. In the second case,[46] experiments were conducted at room temperatures in 500 Torr nitrogen, with metered portions of the flow picking up 0.25-0.75 Torr ozone, which was then almost fully dissociated by the excimer laser beam, and the resulting oxygen atoms recombined through three-body collisions with nitrogen.

Numerical simulation of gas conditions of the shock tube experiments[45] is conducted here for a 0.5% O–99.5% Ar mixture initially at 40 cm Hg and 2400 K. Note that the argon temperature increased somewhat due to heat release in recombination, but that increase was only about 20 K. As the reference point, the first computation was conducted with the dissociation reactions turned off. In this case, only the recombination process, driven by the recombination rate at that temperature, impacts the oxygen mole fractions. This makes the result comparable to the recombination-only DSMC calculation of Ref. 8. For full compatibility, these recombination-only computations have used the recommended[8] oxygen-argon recombination rate with $A_r = 1.1 \times 10^{-44}$ m^6/(molecule^2/s). The comparison with Ref. 8 is given in Fig. 4(a), where the present results are labeled "Modeling, R," and those of Ref. 8, "Koura (1994)." The plot shows the temporal relaxation of the ratio of the initial number density of oxygen atoms, $n_O(0)$, to the instantaneous time-dependent oxygen atom density $n_O(t)$. Clearly, there is good agreement, and a small difference is attributed to the statistical scatter inherent in DSMC.
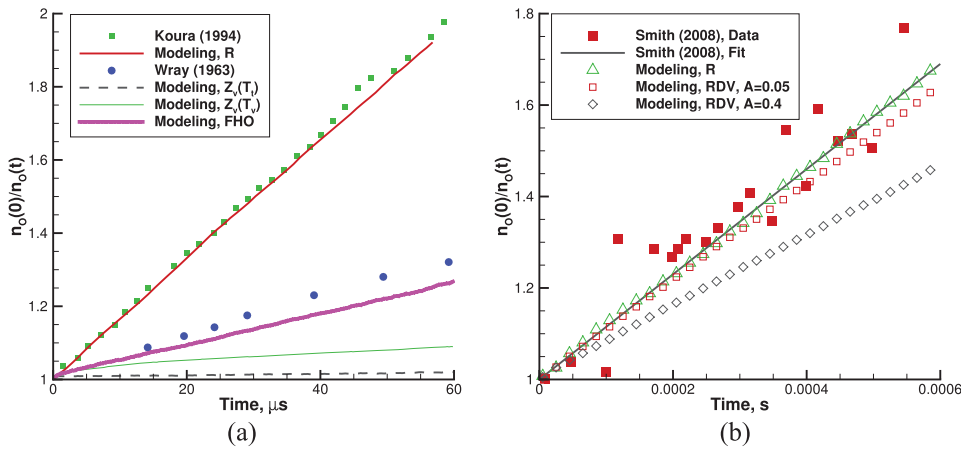
FIG. 4. Temporal relaxation of O population in Ar (left) and N_2 (right) baths.

Comparison with the measurements of Ref. 45 for a recombining-dissociating gas is also shown in Fig. 4(a). In this case, the reaction rates from Tables I and II were used. The experimental data are labeled "Wray (1963)." Note that the experimental points are much lower than the results for the recombination-only flow. The much slower recombination process in the experiment is attributed primarily to the dissociation of newly created atoms. Even though the translation-rotation temperature of the gas is relatively low, 2400 K, it is still sufficient to dissociate oxygen molecules from the upper vibrational levels. The population of such molecules is disproportionally high since the recombination mostly leads to the formation of vibrationally excited molecules.

The present baseline simulation is denoted "Modeling, $Z_v(T_t)$." In the baseline setup, the vibration-translation (VT) energy transfer in O_2–Ar collisions was modeled using the conventional LB approach with the translational temperature dependent vibrational relaxation number $Z_v \equiv Z_v(T_v)$ determined by the Millikan-White empirical correlation[47] with Park's high temperature correction.[48] As clearly seen in Fig. 4(a), the mole fraction ratio for the baseline bias model is much lower than that in the experiment. The difference is mostly due to the inapplicability of the standard LB procedure in this case. The VT energy transfer rate computed using the translational temperature of 298 K is negligible compared to the recombination and dissociation rates, and there is no de-excitation of oxygen molecules that populate high vibrational levels after recombination. As the result, the recombined molecules quickly dissociate, and the population of O_2 becomes almost frozen after 40 μs.

In order to overcome this obvious issue, a simple correction to the LB approach has been used, where the Millikan-White expression is now based on the vibrational and not translational temperature. The result, shown as "Modeling, $Z_v(T_v)$," indicates significant improvement as compared to the standard LB approach. Still, the computed rate of molecular oxygen formation visibly underpredicts the measured rate. In an attempt to alleviate the problem, a state-to-state 3D Forced Harmonic Oscillator (FHO) model[49] is also used for the VT energy transfer. The results obtained using this model are denoted "Modeling, FHO." The 3D FHO model has been shown to match trajectory calculations for all vibrational levels[49] and is believed to provide adequate

accuracy to the VT energy exchange of diatomic molecules. As shown in Fig. 4(a), the use of that model results in good agreement with the experimental data. The computed O_2 formation rate is approximately 20% lower than the measured rate. There may be several reasons for the difference. First, the bias dissociation model overpredicts its Arrhenius fit for O_2–Ar by about 10% at temperatures below 3000 K. Second, the equilibrium constant[42] becomes less accurate—and generally too high—at temperatures below 3000 K. Finally, the recombination model proposed in this work, while accurate in providing detailed balance near equilibrium, may be less accurate for highly nonequilibrium flows, where it is not clear how well the assignment of internal energies of dissociating molecules to molecules created after the recombination reproduces the actual reaction cross sections.

The second series of validation computations have been conducted for the conditions that reproduce those of the Ref. 46 experiments. Atomic oxygen, initially at a partial pressure of 0.57 Torr, is modeled in 504 Torr N_2 at a room temperature of 298 K (this temperature increased with time to 302 K because of the recombination). The major difficulty of comparing to the data[46] is the largely unknown oxygen dissociation rate at such a low temperature. In this case, it is reasonable to use the recommended[46] oxygen in the nitrogen recombination rate of $k_r = 1.9 \times 10^{-45}$ m^6/(molecule^2/s) and calculate the corresponding dissociation rate using the 300 K equilibrium constant of 5×10^{-56} molecule/m^3. In this case, the parameter A_d of the bias dissociation model is approximately 0.05, and not 0.4 valid for higher temperatures.

Comparison of the computed atomic oxygen mole fraction with the experiment[46] is therefore given in Fig. 4(b) for three different cases: the recombination-only case ("Modeling, R"), the recombination-dissociation case with $A_d = 0.4$ ("Modeling, RDV, A=0.4"), and the recombination-dissociation case with $A_d = 0.05$ ("Modeling, RDV, A=0.05"). The 3D FHO model[50] was used for the VT energy transfer. As expected, the recombination-only relaxation follows closely the analytical slope of the fitted experimental rate of $k_r = 1.9 \times 10^{-45}$ m^6/(molecule^2/s). The dissociation predictably decreases that slope. Note that the experimental fit proposed in Ref. 46 does not take into account the possibility of the concurrent dissociation from high vibrational levels, and

thus the difference between the experimental fit and the full dissociation-recombination model could be expected. That difference is small, however, for the realistic dissociation rate of $A_d = 0.05$. The use of the high-temperature dissociation rate results in the underprediction of the experimental slope by over 30%.

IX. CONCLUSIONS

Kinetic simulations of high temperature flows often need fast and reliable models that capture the key physics and that can be used on reactions for which detailed cross-sectional information is not available. The bias dissociation model is unique in needing no *a priori* assumption of an Arrhenius rate coefficient and essentially no adjustable parameters (its pre-exponential factor is on the order of unity). It reproduces vibration-dissociation coupling, equilibrium, and nonequilibrium behavior as a natural consequence of its physics-based cross-sectional function and just a simple chemistry-based assessment of whether the reaction will be strongly favored or not. One disadvantage of the model used to be the lack of a compatible recombination model.

To fill this gap, a recombination model is developed in this work suitable for the direct simulation Monte Carlo method and compatible with the bias dissociation model. The model captures the temperature dependence of the equilibrium reaction constant and satisfies the detailed balance requirement at equilibrium. The recombination probability is derived using the collision theory for chemical reactions, and the rotational and vibrational modes of newly created molecules are populated with the corresponding levels of most recently dissociated molecules. The model is straightforward to implement and was shown to provide reasonable agreement with results of previous numerical simulations and experiments on atomic oxygen recombination.

The approach to modeling the recombination process is general enough to be used for many other dissociation models. While the present implementation assumes the independence of the internal energy states of molecule created after recombination on the chemical species of the third particle, that dependence may easily be incorporated. It would only require the extension of the array that stores rotational and vibrational levels of dissociated molecules to include the information about the third-particle species. Note also that the present implementation considers only the recombination of two atoms into a diatomic molecule. While the extension to the dissociation and recombination of polyatomic molecules is possible, it may be difficult due to significantly higher memory requirements for the array of internal states, as well as the need to take into consideration the internal states of the molecular products of dissociating polyatomic molecules and molecular reactants that participate in recombination.

ACKNOWLEDGMENTS

[1] G. A. Bird, "Approach to translational equilibrium in a rigid sphere gas," Phys. Fluids **6**(10), 1518–1519 (1963).

[2] G. A. Bird, *Molecular Gas Dynamics and the Direct Simulation of Gas Flows* (Clarendon Press, Oxford, 1994).

[3] M. S. Ivanov and S. F. Gimelshein, "Computational hypersonic rarefied flows," Annu. Rev. Fluid Mech. **30**(1), 469–505 (1998).

[4] G. A. Bird, "Monte Carlo simulations in an engineering context," Rarefied Gas Dyn.: Theory Simul., Prog. Astronaut. Aeronaut. **74**, 239–255 (1981).

[5] G. A. Bird, "New chemical reaction model for direct simulation Monte Carlo studies," Rarefied Gas Dyn.: Theory Simul., Prog. Astronaut. Aeronaut. **159**, 185–196 (1994).

[6] D. Hash and H. Hassan, "Direct simulation with vibration-dissociation coupling," AIAA Paper No. 92-2875, 1992.

[7] B. L. Haas and I. D. Boyd, "Models for direct Monte Carlo simulation of coupled vibration-dissociation," Phys. Fluids A **5**, 478–489 (1993).

[8] K. Koura, "A set of model cross sections for the Monte Carlo simulation of rarefied real gases: Atom-diatom collisions," Phys. Fluids A **6**, 3473–3486 (1994).

[9] M. A. Gallis and J. K. Harvey, "Modelling of chemical reactions in hypersonic rarefied flow with the direct simulation Monte Carlo method," J. Fluid Mech. **312**, 149–172 (1996).

[10] I. Boyd, "A threshold line dissociation model for the direct simulation Monte Carlo method," Phys. Fluids **8**, 1293–1300 (1996).

[11] Ye. Bondar, N. Gimelshein, S. Gimelshein, M. Ivanov, and I. Wysong, "On the accuracy of DSMC modeling of rarefied flows with real gas effects," AIP Conf. Proc. **762**, 607–613 (2005).

[12] N. E. Gimelshein, D. A. Levin, and S. F. Gimelshein, "Hydroxyl formation mechanisms and models in high-altitude hypersonic flows," AIAA J. **41**(7), 1323–1331 (2003).

[13] T. E. Schwartzentruber and I. D. Boyd, "Progress and future prospects for particle-based simulation of hypersonic flow," Prog. Aerosp. Sci. **72**, 66–79 (2015).

[14] R. D. Levine, *Molecular Reaction Dynamics* (Cambridge University Press, Cambridge, 2005).

[15] A. Alexeenko and S. F. Gimelshein, "Direct simulation Monte Carlo," in *The Handbook of Fluid Dynamics*, 2nd ed. (CRC Press, 2016), Chap. V.6.

[16] Z. Li, N. Parsons, and D. A. Levin, "A study of internal energy relaxation in shocks using molecular dynamics based models," J. Chem. Phys. **143**, 144501 (2015).

[17] A. Kashkovsky, "3D DSMC computations on a heterogeneous CPU-GPU cluster with a large number of GPUs," AIP Conf. Proc. **1628**, 192 (2014).

[18] M. A. Gallis, J. R. Torczynski, S. J. Plimpton, D. J. Rader, and T. Koehler, "Direct simulation Monte Carlo: The quest for speed," AIP Conf. Proc. **1628**, 27 (2014).

[19] R. Jambunathan and D. A. Levin, "A hybrid CPU-GPU parallel octree direct simulation Monte Carlo approach," AIAA Paper No. 2015-3057, 2015.

[20] A. Kashkovsky, A. Shevyrin, A. Molchanova, and Ye. Bondar, "Implementation of the real gas effects model in SMILE-GPU DSMC numerical tool," in 30th International Symposium On Rarefied Gas Dynamics, University of Victoria, Victoria, BC, Canada, 10–15 July 2016.

[21] R. Jaffe, D. Schwenke, and G. Chaban, "Vibrational and rotational excitation and dissociation in N_2–N_2 collisions from accurate theoretical calculations," AIAA Paper No. 2010-4517, 2010.

[22] N. Parsons, T. Zhu, D. A. Levin, and A. C. T. van Duin, "Development of DSMC chemistry models for nitrogen collisions using accurate theoretical calculations," AIAA Paper No. 2014-1213, 2014.

[23] P. Valentini, T. E. Schwartzentruber, J. D. Bender, I. Nompelis, and G. V. Candler, "Direct molecular simulation of nitrogen dissociation based on an *ab initio* potential energy surface," Phys. Fluids **27**, 086102 (2015).

[24] M. Kulakhmetov, M. Gallis, and A. Alexeenko, "*Ab initio*-informed maximum entropy modeling of rovibrational relaxation and state- specific dissociation with application to the $O_2 + O$ system," J. Chem. Phys. **144**, 174302 (2016).

[25] D. A. Andrienko and I. D. Boyd, "Rovibrational energy transfer and dissociation in O_2–O collisions," J. Chem. Phys. **144**, 104301 (2016).

[26] A. Munafo, Y. Liu, and M. Panesi, "Modeling of dissociation and energy transfer in shock-heated nitrogen flows," Phys. Fluids **27**, 127101 (2015).

[27] I. J. Wysong and S. F. Gimelshein, "Comparison of DSMC reaction models with QCT reaction rates for nitrogen," in 30th International Symposium On Rarefied Gas Dynamics, University of Victoria, Victoria, BC, Canada, 10–15 July 2016.

[28] R. Jaffe, D. Schwenke, and G. Chaban, "Theoretical analysis of N_2 collisional dissociation and rotation-vibration energy transfer," AIAA Paper No. 2009-1569, 2009.

[29] J. Kim and I. Boyd, "Monte Carlo simulation of nitrogen dissociation based on state-resolved cross sections," Phys. Fluids **26**, 012006 (2014).

[30] D. C. Wadsworth and I. J. Wysong, "Vibrational favoring effect in DSMC dissociation models," Phys. Fluids **9**, 3873–3884 (1997).

[31] I. B. Sebastio and A. Alexeenko, "Consistent post-reaction vibrational energy redistribution in DSMC simulations using TCE model," Phys. Fluids **28**, 107103 (2016).

[32] C. Borgnakke and P. S. Larsen, "Statistical collision model for Monte Carlo simulation of polyatomic gas mixture," J. Comput. Phys. **18**, 405–420 (1975).

[33] I. D. Boyd, "Analysis of vibration-dissociation-recombination processes behind strong shock waves of nitrogen," Phys. Fluids A **4**, 178–185 (1992).

[34] S. F. Gimelshein and M. S. Ivanov, "Simulation of chemically reacting gas flow using majorant frequency scheme of DSMC," Rarefied Gas Dyn.: Theory Simul., Prog. Astronaut. Aeronaut. **159**, 218–233 (1994).

[35] G. A. Bird, "The Q-K model for gas-phase chemical reaction rates," Phys. Fluids **23**, 106101 (2011).

[36] M. Uddi, N. Jiang, I. V. Adamovich, and W. R. Lempert, "Nitric oxide density measurements in air and air/fuel nanosecond pulse discharges by laser induced fluorescence," J. Phys. D: Appl. Phys. **42**(7), 075205 (2009).

[37] C. R. Lilley and M. N. Macrossan, "A macroscopic chemistry method for the direct simulation of gas flows," Phys. Fluids **16**, 2054–2066 (2004).

[38] I. V. Adamovich, S. O. Macheret, C. Treanor, and J. W. Rich, "Vibrational relaxation and dissociation behind shock waves. Part 1: Kinetic rate models," AIAA J. **33**(6), 1064–1069 (1995).

[39] M. S. Ivanov and S. V. Rogasinsky, "Analysis of the numerical techniques of the direct simulation Monte Carlo method in the rarefied gas dynamics," Russ. J. Numer. Anal. Math. Modell. **3**(6), 453–465 (1988).

[40] N. E. Gimelshein, S. F. Gimelshein, D. A. Levin, M. S. Ivanov, and I. J. Wysong, "Reconsideration of DSMC models for internal energy transfer and chemical reactions," AIP Conf. Proc. **663**, 349–357 (2003).

[41] L. Onsager, "Reciprocal relations in irreversible processes. I," Phys. Rev. **37**, 405–426 (1931).

[42] W. G. Vincenti and C. H. Kruger, *Introduction to Physical Gas Dynamics* (Krieger, 1965).

[43] F. T. Smith, "Chemical reactions in high temperature gases as collision processes," in *Kinetic Processes in Gases and Plasmas*, edited by A. R. Hochstim (Academic Press, New York, 1969), pp. 257–280.

[44] M. S. Ivanov, G. N. Markelov, and S. F. Gimelshein, "Statistical simulation of the transition between regular and Mach reflection in steady flows," Comput. Math. Appl. **35**(1-2), 113–126 (1998).

[45] K. L. Wray, "Shock-tube study of the recombination of O atoms by Ar catalysts at high temperatures," J. Chem. Phys. **38**, 1518 (1963).

[46] G. P. Smith and R. Robertson, "Temperature dependence of oxygen atom recombination in nitrogen after ozone photolysis," Chem. Phys. Lett. **458**, 6–10 (2008).

[47] R. C. Millikan and D. R. White, "Systematics of vibrational relaxation," J. Chem. Phys. **39**, 3209–3213 (1963).

[48] C. Park, "Problems of rate chemistry in the flight regimes of aeroassisted orbital transfer vehicles," Therm. Des. Aeroassisted Orbital Transfer Veh., Prog. Astronaut. Aeronaut. **6**, 511–537 (1985).

[49] I. V. Adamovich and J. W. Rich, "Three-dimensional nonperturbative analytic model of vibrational energy transfer in atom-molecule collisions," J. Chem. Phys. **109**, 7711–7723 (1999).

[50] I. V. Adamovich, "Three-dimensional analytic model of vibrational energy transfer in molecule-molecule collisions," AIAA J. **39**, 1916–1925 (2001).